Atmos. Chem. Phys. Discuss., 14, 14889–14931, 2014
www.atmos-chem-phys-discuss.net/14/14889/2014/
doi:10.5194/acpd-14-14889-2014

Atmospheric Chemistry and Physics Discussions

Aerosol hygroscopicity and CCN activity obtained from a combination analysis based on size-resolved CCN and aerosol chemical composition observations during the AC^{3}Exp13 campaign

F. Zhang[1], Z. Li[1,2], R. J. Li[1], L. Sun[3], C. Zhao[1], P. C. Wang[3], Y. L. Sun[3], Y. N. Li[1], X. G. Liu[4], J. X. Li[5,6], P. R. Li[5], G. Ren[5], and T. Y. Fan[1]

[1]College of Global Change and Earth System Science, Beijing Normal University, Beijing 100875, China
[2]Earth System Science Interdisciplinary Center and Department of Atmospheric and Oceanic Science, University of Maryland, College Park, Maryland, USA
[3]State Key Laboratory of Atmospheric Boundary Layer Physics and Atmospheric Chemistry, Institute of Atmospheric Physics, Chinese Academy of Sciences, Beijing 100029, China
[4]State Key Laboratory of Water Environment Simulation, School of Environment, Beijing Normal University, Beijing 100875, China
[5]Weather Modification Office of Shanxi Province, Taiyuan 030032, China

[6]Key Laboratory for Aerosol-Cloud-Precipitation of China Meteorological Administration, Nanjing University of Information Science and Technology, Nanjing 210044, China

Received: 22 April 2014 – Accepted: 22 May 2014 – Published: 6 June 2014

Correspondence to: Z. Li (zli@atmos.umd.edu)

Published by Copernicus Publications on behalf of the European Geosciences Union.

ACPD
14, 14889–14931, 2014

Abstract

Aerosol hygroscopicity and cloud condensation nuclei (CCN) activity under clean conditions and polluted events are investigated based on size-resolved CCN and aerosol chemical composition observations during the Aerosol-CCN-Cloud Closure Experiment (AC^3Exp) campaign conducted at Xianghe, China in summer 2013. About 14–22 % of aerosol particles during the campaign are of externally mixed CCN-inactive particles that cannot serve as CCN under atmospheric typical supersaturation (SS) of ~ 0.4 %. A high sensitivity of Maximum activation fractions (MAF) to SS under polluted conditions has been observed. The pollutants can cause a maximum MAF decrease of 25–30 % (at SS = 0.08 %). Hygroscopicity parameter kappa (κ) are about 16–35 % lower under polluted conditions than under clean conditions for particles in accumulation size range (80–180 nm); however, for particles in nucleation or Aitken size range (30–60 nm), κ is slightly higher under polluted conditions. A non-parallel observation (NPO) CCN closure study shows low correlation coefficient between estimated and observed CCN number concentrations (N_{CCN}). About 30–40 % uncertainties in N_{CCN} prediction are associated with the changes of particle composition. A case study shows that CCN activation ratio (AR) increased with the increase of condensation nuclei (CN) number concentrations (N_{CN}) in relatively clean days. In the case, AR exhibited good correlation with κ_{chem}, which is calculated from chemical volume fractions, due to particles mainly composed of soluble inorganics. On the contrary, AR declined with increase of N_{CN} during polluted events when particles composed mostly of organics. Meanwhile, AR is closely related to f_{44}, which is the fraction of total organic mass signal at m/z 44 and closely associated with particle organic oxidation level. Our study highlights the importance of aerosols chemical composition on determining the activation properties of aerosol particles, underlining the importance of long-term observation of CCN under different atmospheric environments, especially those with heavy pollution and high CN number concentrations.

ACPD
14, 14889–14931, 2014

1 Introduction

Indirect influence of aerosol particles on the radiative balance of the atmosphere through changes in cloud droplet number and persistence of clouds (Twomey, 1974; Albrecht, 1989), carries the largest uncertainty amongst the presently known causes of radiative forcing (IPCC, 2007, 2013). Thus, better understanding of aerosol formation, growth and activation is essential.

Field and laboratory experiments have been conducted with the aim of better characterizing the particle physical and chemical parameters impacting on cloud condensation nuclei (CCN) activation. Studies have addressed the relative importance of the size distribution, particle composition and mixing state in determining CCN activation, but there are disagreements on the relative importance of these parameters (e.g. Roberts et al., 2002; Feingold, 2003; Ervens et al., 2005; Mircea et al., 2005; Dusek et al., 2006a; Anttila and Kerminen, 2007; Hudson, 2007; Quinn et al., 2008; Zhang et al., 2008; Deng et al., 2013; Ma et al., 2013). CCN closure studies are a useful approach to test our knowledge of the controlling physical and chemical factors and help verify experimental results. CCN number concentration, N_{CCN}, is usually predicted from measured aerosol properties such as size distribution and composition or hygroscopicity based on Köhler theory. The closure between the measured and estimated N_{CCN} is often able to achieve in the background atmosphere without heavy pollutions (Chuang et al., 2000; Dusek et al., 2003; VanReken et al., 2003; Rissler et al., 2004; Gasparini et al., 2006; Stroud et al., 2007; Bougiatioti et al., 2009).

In urban/polluted areas, the particle size distribution is more complex with various composition of air mass (Lee et al., 2003; Alfarra et al., 2004; Zhang et al., 2004a; Salcedo et al., 2006). The particle activation is affected by composition and mixing state of the aerosol particles. It has been demonstrated that particles are more difficult to be activated during biomass burning plumes (Mircea et al., 2005; Lee et al., 2006; Clarke et al., 2007; Rose et al., 2010, 2011; Paramonov et al., 2013; Lathem et al., 2013). Also, their activation ratios were reduced by secondary organics formed from oxidation

ACPD
14, 14889–14931, 2014

of common biogenic emissions (VanReken et al., 2005; Varutbangkul et al., 2006; Mei et al., 2013) and black carbon (Dusek et al., 2006b; Kuwata et al., 2007). Other organic components (e.g. organic acids) are shown to activate more easily (Raymond and Pandis, 2002; Hartz et al., 2006; Bougiatioti et al., 2011), but still much less than inorganic species. Therefore, heavy polluted areas represent one of the most challenging cases to test the understanding of parameters controlling CCN activation and growth. Furthermore, the main uncertainty in predicting the magnitude of the global aerosol indirect effects arises from those regions with the influence of urban emissions (Sotiropoulou et al., 2007). The study of aerosol-CCN closure and relationships inside and in the outflow of heavily polluted areas is thus important.

East Asia, especially the Jing (Beijing)–Jin (Tianjin)–Ji (Hebei) region, is a fast developing and densely populated region including numerous megacities, where anthropogenic aerosol emissions have increased significantly over recent years (Streets et al., 2008) and where aerosol loading is high and chemical composition is complex (Li et al., 2007a; Xin et al., 2007). The high aerosol loading would have significant influence on radiative properties, cloud microphysics and precipitation (Xu, 2001; Li et al., 2007b; Xia et al., 2007; Rosenfeld et al., 2007; Lau et al., 2008; Li et al., 2011).

Field measurements of CCN have been made in East Asia where megacities are likely to be major sources of pollutants and CCN (Yum et al., 2007; Rose et al., 2008; Gunthe et al., 2009; Yue et al., 2011; Liu et al., 2011; Zhang et al., 2012; Deng et al., 2011; Leng et al., 2013). Despite the significant accomplishments achieved by these studies, limitations and uncertainties exist. As a recent example for the region of interest, Deng et al. (2011) over predicted the concentration of CCN at a site in the North China Plain by 19 % when compared with direct measurements.

The aim of this paper is to study the CCN activity under high aerosol loading in the polluted regions and examine the impacts of particle size and chemical composition on CCN activation ratio (AR) to the proxy of total aerosol particles in the atmosphere. We applied a CDF fit model to both clean and polluted aerosols to probe the influences of size distribution, heterogeneity of chemical composition, and mixing state on CCN

ACPD
14, 14889–14931, 2014

activity. The hygroscopicity parameter is derived using Köhler theory to study aerosols hygroscopicity during clean days and polluted events. In the CCN closure study, in addition to the parallel observation (PO) closure test, we also employ the CDF active curve fit method to non-simultaneously CN and CCN observation (namely non-parallel observation (NPO) closure test) to estimate N_{CCN}. Finally, the relationship between AR and aerosol physical and chemical properties is examined to further understand the different behavior of CCN activity under background condition and during polluted events.

2 Measurement and data

An intensive campaign, named Aerosol-CCN-Cloud Closure Experiment (AC^3Exp), was conducted during June and July of 2013 at the Xianghe Atmospheric Observatory (39.798° N, 116.958° E; 35 m a.s.l.), located about 60 km southeast of the Beijing metropolitan area. This site is surrounded by agricultural land, densely occupied residences and light industry. Sitting between two megacities (with Beijing to the northwest and Tianjin to the southeast) and less than 5 km west of the local town center (with a population of 50 000), the site experiences frequent pollution plumes. Depending on the wind direction, instruments at the Xianghe site detect pollutants of urban, rural, or mixed origins, experiencing both fresh biomass burning emissions and advected aged aerosols. More information about the measurement location and meteorological conditions has been described by Li et al. (2007, 2011).

2.1 Instrument and measurement

In the campaign, aerosol particle size distribution (10–500 nm) and bulk CCN activation were measured from 1 to 25 June 2013. Size-resolved CCN was measured from 25 June to 21 July 2013 and aerosol chemical composition was measured from 31 May to 30 June 2013. The aerosol inlet for the size distribution measurements was equipped

ACPD
14, 14889–14931, 2014

with a TSI Environmental Sampling System (Model 3031200), which consists of a standard PM_{10} inlet, a sharp-cut PM_1 cyclone, and a bundled nafion dryer. After dried through the nafion bundle, the sample flow was sent into a Scanning Mobility Particle Sizer (SMPS, TSI 3034) for the aerosol size distribution measurements (10–500 nm). Meanwhile, the CCN number concentrations (N_{CCN}) at different super-saturations were measured, using a continuous-flow CCN counter from Droplet Measurement Technologies – Cloud Condensation Nuclei Counter (DMT-CCN_C; Lance et al., 2006). Each CCN measurement cycle included three supersaturations: 0.2, 0.5 and 0.8 %. The scanning times for those super-saturations were set as 7, 5, and 5 min, respectively.

The size-resolved CCN efficiency spectra were measured by coupling the same DMT-CCN_C used with a SMPS system (DMA; TSI 3081, CPC; TSI 3776) (Rose et al., 2008). In this setup the particles are rapidly dried upon entering the DMA. Thus, size selection is effectively performed under dry conditions, and the relative deviations in particle diameter should be < 1 % except for potential kinetic limitations (Mikhailov et al., 2009). The sample flow exiting the DMA was split into two parts, with 0.3 lpm for the CPC and 0.5 lpm for the CCN_C. The DMA, controlled by the TSI-AIM software, scanned one size distribution every five minutes with a size range between 10 and 700 nm. The CCN_C was operated at a total flow rate of 0.5 lpm with the sheath-to-aerosol flow ratio of 10. During the campaign, the averaging temperature and pressure as measured by the CCN_C sensors were $(23.5 \pm 1.6)\,^{\circ}C$ and (985.5 ± 3.6) hPa. The deviations were determined by the measurement uncertainties. For each CCN measurement cycle, SS was set to 5 different values: 0.08, 0.11, 0.23, 0.42, and 0.80 %. The completion of a full measurement cycle took 60 min (20 min for the SS = 0.08 % and 10 min for each of the rests). The supersaturations of CCN_C were calibrated with ammonium sulfate both before and after the campaign, following Rose's procedures (Rose et al., 2008).

The measurement of non-refractory submicron (NR-PM1) aerosol species including organics, sulfate, nitrate, ammonium, and chloride with an Aerodyne Aerosol Chemical Speciation Monitor (ACSM) (Sun et al., 2012) is also conducted. The aerosol sampling

ACPD
14, 14889–14931, 2014

setup and the ACSM operations were same as those in Sun et al. (2012). In addition to the ACSM, the black carbon (BC) was simultaneously measured by a BC analyzer (Aethalometer, Model AE22, Magee Scientific Corporation). During the experiment period, the campaign area was generally hot and wet, with an average temperature of 23.6 °C and an average ambient relative humidity (RH) of 72.3 %.

2.2 Data

The raw CCN data for both bulk and size-resolved CCN measurements were firstly filtered according to the instrument recorded parameters (e.g. temperature and flow). A multiple charge correction is applied for each CN size distribution spectrum by TSI-AIM software. The CCN activation ratio (AR) is calculated based on the ratio of N_{CCN}/N_{CN}. In order to examine the CCN activity under clean and polluted days, we classified the size-resolved CCN efficiency data as polluted and background conditions with CN number concentration $N_{CN} > 15\,000\,cm^{-3}$ and $< 15\,000\,cm^{-3}$ respectively. Here, the background refers to a regional background condition which represents a well-mixed atmosphere without influenced by local emissions. Bulk measurement of total CCN number concentrations at SS of 0.2, 0.5 and 0.8 % could lead to considerable underestimation of CCN under polluted conditions (Deng et al., 2011) due to water depletion inside the column (Lathem and Nenes, 2011). Therefore, in this study the data points with $N_{CN} > 25\,000\,cm^{-3}$ were excluded. In the closure study, CCN size distributions were calculated by multiplying the fitted CCN efficiency spectra (3-parameter CDF fit, Table 1) with the aerosol particle number size distribution. Total N_{CCN} was obtained by integrating the CCN over whole size range. The mass concentrations and mass spectra were processed using ACSM standard data analysis software (v 1.5.1.1). The detailed procedures for the data analysis have been described in Ng et al. (2011) and Sun et al. (2012).

ACPD
14, 14889–14931, 2014

3 Theory

As proposed by Petters and Kreidenweis (2007), κ can be used to describe the influence of chemical composition on the CCN activity of aerosol particles, i.e. their ability to absorb water vapor and act as CCN. Based on Köhler theory (Köhler, 1936), κ relates the dry diameter of aerosol particles to the critical water vapor SS, i.e. the minimum SS required for cloud droplet formation. According to measurements and thermodynamic models, κ is zero for insoluble materials like soot or mineral dust, however, their hygroscopicity would be changed due to the aging process of the soot and mineral dust and the κ value is thus > 0. κ is 0.1 for secondary organic aerosols, 0.6 for ammonium sulfate and nitrate, 0.95–1 for sea salt (Niedermeier et al., 2008), and 1.28 for sodium chloride aerosols. The effective hygroscopicity of mixed aerosols can be approximated by a linear combination of the κ values of the individual chemical components weighted by the volume or mass fractions, respectively (Kreidenweis et al., 2008; Gunthe et al., 2009). In this study, we calculated κ based on both size-resolved CCN measurements and chemical composition observations during the campaign. The theory and method to derived κ are described below.

3.1 Derivation of κ_a and κ_{cut}

Particle hygroscopicity κ were derived from the measured size resolved CCN activated fraction using κ-Köhler theory (Petters and Kreidenweis, 2007). In κ-Köhler theory, the water vapor saturation ratio over an aqueous solution droplet S is given by:

$$S = \frac{D^3 - D_p^3}{D^3 - D_p^3(1-\kappa)} \exp\left(\frac{4\sigma_w M_w}{RT\rho_w D}\right) \quad (1)$$

where D is the droplet diameter, D_p is the dry diameter of the particle, M_w is the molecular weight of water, σ_w is the surface tension of pure water, ρ_w is the density of water, R is the gas constant, and T is the absolute temperature. When κ is greater than 0.1,

ACPD
14, 14889–14931, 2014

it can be conveniently derived as:

$$\kappa = \frac{4A^3}{27D_p^3 S_c^2} \quad (2)$$

$$A = \frac{4\sigma_w M_w}{RT\rho_w} \quad (3)$$

where S_c is the particle critical supersaturation and is derived using the approach described by Rose et al. (2008). The characteristic S_c of the size selected CCN is represented by the supersaturation at which AR reaches 50 %. For parameters listed above, $T = 298.15\,\mathrm{K}$, $R = 8.315\,\mathrm{J\,K^{-1}\,mol^{-1}}$ (gas constant), $\rho_w = 997.1\,\mathrm{kg\,m^{-3}}$, $M_w = 0.018015\,\mathrm{kg\,mol^{-1}}$ and $\sigma_w = 0.072\,\mathrm{J\,m^{-2}}$. Note that values derived from CCN measurement data through Köhler model calculations assuming the surface tension of pure water have to be regarded as "effective hygroscopicity parameters" that account not only for the reduction of water activity by the solute ("effective Raoult parameters") but also for surface tension effects (Petters and Kreidenweis, 2007).

In this study, a parameter κ_a, which characterizes the average hygroscopicity of CCN-active particles in the size range around activated diameters (D_a), is calculated from the data pairs of SS and D_a based on the κ-Köhler theory. κ_a is better suited for comparison with values predicted from ACSM measurements, because κ_a is not influenced by CCN-inactive particles consisting mostly of insoluble and refractory materials like mineral dust and soot, which are not or less efficiently detected by ACSM. Similarly, a parameter κ_{cut} is also derived from the data pairs of SS and a critical dry particle diameter D_{cut} based on the κ-Köhler theory, which characterizes the average hygroscopicity of aerosol particles in the size range around D_{cut}. Note the D_{cut} is the diameter when the AR = 50 % regardless of MAF < 1 or MAF = 1. Whereas, D_a is the diameter when the AR = MAF/2 (see Sect. 4.1). The discrepancy of D_{cut} and D_a can reflect the mixing state and chemical heterogeneity of aerosol particles.

ACPD
14, 14889–14931, 2014

3.2 Derivation of κ_{chem}

For a given internal mixture, κ can be predicted by a simple mixing rule on the basis of chemical volume fractions ε_i (Petters and Kreidenweis, 2007; Gunthe et al., 2009).

$$\kappa_{chem} = \sum_i \varepsilon_i \kappa_i \quad (4)$$

where, κ_i and ε_i are the hygroscopicity parameter and volume fraction for the individual (dry) component in the mixture with i the number of components in the mixture. We derive ε_i from the particle chemical composition measured by ACSM. Measurements from ACSM show that the composition of submicron particles was dominated by organics, followed by nitrate, ammonium and sulfate. The contribution of chloride was negligible (with volume fraction of about $< 2\,\%$). The analysis of anion and cation balance suggests that anionic species (NO_3^-, SO_4^{2-}) were essentially neutralized by NH_4^+ over the relevant size range. For refractory species, BC represented a negligible fraction of the total submicron aerosol volume (less than about 3 %), and the contribution of sea salt and dust are also expected to be negligible for the size range of < 500 nm. Therefore, aerosols within the size range of 10–500 nm examined were mainly consisting of Organics, $(NH_4)_2SO_4$, and NH_4NO_3. The particle hygroscopicity is thus the volume average of the three participating species:

$$\kappa_{chem} = \kappa_{org} \cdot \varepsilon_{org} + \kappa_{(NH_4)_2SO_4} \cdot \varepsilon_{(NH_4)_2SO_4} + \kappa_{NH_4NO_3} \cdot \varepsilon_{NH_4NO_3} \quad (5)$$

The values of κ are 0.1, 0.67 and 0.61 for Organics, $(NH_4)_2SO_4$, and NH_4NO_3, respectively derived from previous laboratory experiments (Petters et al., 2007). Species volume fractions were derived from mass concentrations and densities of participating species. The densities of $(NH_4)_2SO_4$ and NH_4NO_3 are 1770 and 1720 $kg\,m^{-3}$, respectively. And the density of organics is 1200 $kg\,m^{-3}$ (Turpin et al., 2001).

ACPD
14, 14889–14931, 2014

4 Results and discussion

4.1 CDF fit and parameters derived from the CCN efficiency

The spectra of measured CCN efficiency at both polluted and background conditions were fitted with a cumulative Gaussian distribution function (CDF; Rose et al., 2008):

$$f_{N_{CCN}/N_{CN}} = a\left(1 + \mathrm{erf}\left(\frac{D - D_a}{\sigma_a\sqrt{2}}\right)\right) \quad (6)$$

where, the maximum activated fraction MAF = 2a, the midpoint activation diameter D_a, and the CDF standard deviation σ_a. The parameters were determined for each spectrum. If MAF = 1 by changing parameter "a" to 0.5, the spectrum is characteristic for internally mixed aerosols with homogeneous composition and hygroscopicity of the particles. During the campaign period of AC^{3}Exp 2013, we measured about 1200 size-resolved CCN efficiency spectra (activation curves) for atmospheric aerosols at SS of 0.08 to 0.80 %. Figure 1 shows averaged spectra of measured CCN efficiency at SS of 0.08, 0.11, 0.23, 0.42 and 0.80 % as well as the differences of activation ratios between background and polluted conditions (Fig. 1). The slope of AR with respect to diameter near D_a in Fig. 1 provides information on the heterogeneity of the composition for the size resolved particles. For an ideal case when all CCN-active particles have the same composition and size, a steep change of AR from 0 to MAF would be observed as D reaches D_a. A gradual increase in AR suggests that some of the particles have lower hygroscopicity and/or heterogeneity of the composition and are not able to activate at the given SS than others. From Fig. 1, the slope of AR around D_a during polluted events shows more gentle increase compared with the slope under background conditions, especially at low SS, suggesting that the polluted aerosols have lower hygroscopicity. It shows differences of AR between polluted and background conditions are much larger at SS = 0.08–0.11 % than that at SS = 0.42–0.80 %. This implies that the impact of chemical composition on CCN activity is decreased along with increasing

ACPD
14, 14889–14931, 2014

SS, as has also been found by Kuwata et al. (2008). The pollutants can lead to a maximum decrease of 25–30 % (at SS = 0.08 %) of the activation ratio. The decrease at SS = 0.80 % is about 5 %.

4.1.1 Activation diameter (D_a)

The three parameters (MAF, D_a, and σ) of CCN efficiency spectra derived from the 3-parameter CDF fits as well as D_{cut}, κ_a and κ_{cut} under polluted and clean conditions were also summarized in Table 1. Da_POL and Da_BG in Table 1 are defined as activation diameter under polluted and clean conditions respectively. Dcut_POL and Dcut_BG are defined as cut-off diameter under polluted and clean conditions respectively. As expected, D_a decreased with increasing SS under both background and polluted conditions. Generally, D_a_POL are larger than D_a_BG. Therefore, compared with background aerosols, the polluted particles would be activated at larger diameter at a given SS. However, the effect on D_a has been weakened with the increasing of SS, the difference of D_a_POL and D_a_BG reduced and close to each other at SS = 0.42 % and 0.80 %. Accordingly, D_{cut}_POL and D_{cut}_BG dependence on SS showed similar changes to D_a. In addition, it should be noted that D_{cut} is often larger than D_a derived from the CCN efficiency spectra. Because D_{cut} is defined as the diameter when activation fraction is up to 50 %, but most of cases during the campaign the "MAF/2" is smaller than 50 % due to the externally mixed particle composition. The discrepancy of D_{cut} and D_a just indicated an externally mixed chemical composition of aerosol particles.

4.1.2 Maximum Activated Fraction (MAF)

Generally, aerosols are with more uniform and homogenous chemical composition under background conditions, thus result in a higher MAF. In this study, we observed maximum MAF of 0.98 at SS = 0.11 % under low N_{CN} during the campaign. At SS = 0.08 %, the average MAF was only 0.49 with minimum values as low as 0.1 during those

ACPD
14, 14889–14931, 2014

polluted events. The low MAF observed during the campaign indicate that a substantial portion (1 – MAF, about 14–22 %) of externally mixed CCN-inactive particles consist of only non-hygroscopic species that cannot serve as CCN under typical atmospheric SS of ~ 0.4 %. MAF_POL and MAF_BG in Table 1 are defined as maximum activation fraction under polluted and clean conditions respectively. MAF_POL display significant increase with the increasing of SS; whereas MAF_BG shows a slight increase. This suggests a higher sensitivity of particle MAF to SS under polluted conditions.

4.1.3 CDF standard deviations (σ)

The 3-parameter fit results represent the average activation properties of the aerosol particle fraction. The CDF standard deviations (σ) are general indicators for the extent of external mixing and heterogeneity of particle composition for the investigated aerosol in the size range around D_a. σ_POL and σ_BG in Table 1are defined as CDF standard deviations under polluted and clean conditions respectively. Under ideal conditions, the CDF standard deviations should be zero for an internally mixed, fully monodisperse aerosol with particles of homogeneous chemical compositions. According to Rose et al. (2008), even after correcting for the DMA transfer function, however, calibration aerosols composed of high-purity ammonium sulfate exhibit small non-zero σ values that correspond to ~ 3 % of D_a. It can be attributed to heterogeneities of the water vapor SS profile in the CCNC or other non-idealities, such as DMA transfer function and particle shape effects. Thus, "heterogeneity parameter" values of $\sigma/D_a = 3\,\%$ indicate internally mixed CCN, whereas higher values indicate external mixtures of particles with varying chemical composition and hygroscopicity. σ/Da_POL and σ/Da_BG in Table 1 are defined as heterogeneity parameter under polluted and clean conditions respectively. According to Table 1, σ/D_a_POL and σ/D_a_BG are with values of 20–26 %, which is much higher than 3 % observed for aerosols of homogeneous composition (e.g. pure ammonium sulfate), indicating that the particles were externally mixed with respect to their solute content.

ACPD
14, 14889–14931, 2014

4.2 Derived κ dependence on D_p

Figure 2 shows the dependence of κ_a and κ_{cut} on D_p under both clean and polluted conditions. κ_a_POL and κ_a_BG in Fig. 2 are defined as average hygroscopicity of CCN-active particles in the size range around D_a under polluted and background conditions. κ_{cut}_POL and κ_{cut}_BG are defined as average hygroscopicity of CCN particles in the size range around D_{cut} under polluted and background conditions. For clean days, larger particles were on average more hygroscopic than smaller particles: κ_a_BG and κ_{cut}_BG increased substantially from about 0.4 at 30–60 nm to about 0.6 at size range of 120–180 nm. Our result is consistent with the field results observed in Guangzhou, South China by Rose et al. (2010). However, during polluted events, both κ_a_POL and κ_{cut}_POL did not exhibited significant increase; and larger particles are even less hygroscopic than the smaller particles. Generally, κ for polluted aerosols are about 16–35 % lower than that of clean aerosols for particles in accumulation size range (80–180 nm). The decreased hygroscopisity parameter during polluted events is thus probably due to the aerosols consisted mostly of an external mixture of freshly emitted biomass burning particles (Andreae and Rosenfeld, 2008; Petters et al., 2009; Rose et al., 2010). This can also partially explain the reduction of polluted aerosols activity due to most of the particles within that size range can be served as CCN.

However, for these particles in nucleation or Aitken size range (30–60 nm), κ for polluted particles is slightly higher than clean aerosols. Based on laboratory experiment, Petters et al. (2009) examined the hygroscopic properties of particles freshly emitted from biomass burning. They found that κ was a function of particle size, with 250 nm particles being generally weakly hygroscopic and sub-100 nm particles being more hygroscopic. During the campaign at Xianghe, the biomass burning aerosols are the lead particles. Thus it is safe to conclude that our field observations just confirmed the lab experiment by Petters et al. (2009). Consequently, the impact of pollutions on hygroscopisity of aerosols is complex, which is largely dependent on particle compositions and their mixing state.

ACPD
14, 14889–14931, 2014

4.3 Time series of D_{cut} and κ_{cut}

Figure 3 shows the time series of D_{cut} and derived κ_{cut} at SS of 0.08–0.80 % throughout the campaign. Both D_{cut} and κ_{cut} exhibited pronounced fluctuations during observation period. On 18–19 July, when $N_{CN} < 20\,000\,cm^{-3}$, D_{cut} is relatively low, but the κ_{cut} were enhanced accordingly relative to the campaign average. The changes indicate a decrease in the portion of particulate matter with low hygroscopicity (organic substances) and in the heterogeneity of particles (external mixing). The highly polluted period of 16–17 July 2013 was characterized by intense local biomass burning and very high aerosol number concentrations. During the polluted events, the increase of D_{cut} was pronounced, with apparent enhancement at SS < 0.2 %. Moreover, for all SS, κ_{cut} decreased to below 0.3 during polluted events, indicating a strong increase in the heterogeneity of particles and an increase in the portion of particulate matter with low hygroscopicity (organic substances).

4.4 PDF of D_{cut}, κ_{cut} and κ_{chem}

Figure 4 exhibits the probability distribution function (PDF) of D_{cut} and κ_{cut} under background conditions and during polluted events throughout the campaign. D_{cut}_BG are mainly distributed in the ranges of about 100–200, 100–150, 60–100, 40–60 and 25–50 nm, with mean values of 156.5, 129.3, 84.6, 55.1 and 40.5 nm at SS of 0.08, 0.11, 0.23, 0.42 and 0.80 %, respectively. Obviously, the D_{cut}_BG shows larger variations at low SS than that at high SS. This can be explained by two reasons: one is weaken impact (solute effect) of chemical composition on CCN activity at high SS; the other one is the homogenous composition for these smaller particles according to our previous analysis (with high κ). Variations of D_{cut}_BG are smallest at SS = 0.80 % and largest at SS = 0.08 %. In addition, pollution often increases D_{cut} by several to dozens of nanometer. Generally, PDF of D_{cut}_POL is similar to that of D_{cut}_BG, with large variations at high SS and narrow distribution at low SS. But one can easily find the PDF

ACPD
14, 14889–14931, 2014

for D_{cut}_POL moved several to dozens of nanometer and extended to the side of large particle size at all SS indicating impact by pollutions.

κ_{cut}_BG also presents large variations at each size range around D_p. They are mainly distributed in the ranges of about 0.2–0.6, 0.3–0.6, 0.4–0.6, 0.2–0.6 and 0.2–0.5 at D_{cut} of 163, 137, 90, 55 and 41 nm. It shows that a very small portion of particles are with $\kappa_{cut} < 0.2$ under clean conditions, reflecting that the particles are more hygroscopic. Compared to the PDF of κ_{cut}_BG, κ_{cut}_POL displays more significant variations. Furthermore, the PDF for κ_{cut}_POL is extended or moved to the left side integrally and showing reduced hygroscopicity at all size ranges. The enhanced variations of PDF as well as the decrease in κ_{cut}_POL indicate strong regional pollution with large proportions of externally mixed biomass burning particles in the atmospheric aerosol near Xianghe site.

Figure 5 shows the PDF of derived κ_{chem} under background conditions and during polluted events when assuming a simple approximate mixing rule throughout the campaign. κ_{chem} characterizes the average hygroscopicity of aerosol particles in the size range of < 1 µm ($PM_{1.0}$). The κ_{chem} displays large variations and mainly distributed in the ranges of about 0.3–0.5, with a mean value of 0.38. The influence from pollutions was also indicated, with mean κ_{chem}_POL and κ_{chem}_BG of 0.35 and 0.38 respectively. The average value of κ_{chem} during the campaign is smaller than κ_{cut} and κ_a, as probably implied we have assumed a lower κ_{org} (= 0.1) than it was: organics during the campaign are probably more hygroscopic due to the aging process. On average, continental aerosols tend to cluster around $\kappa = 0.3$ (Andreae and Rosenfeld, 2008; Pringle et al., 2010). Our derived κ during the campaign from size-resolved CCN measurements and aerosol chemical composition measurements by ASCM are considerably higher than previous field observations. The large variation of κ (varying from 0 to 1.2) in our study indicate that particles are characterized by biomass burning influenced aerosols, which has been yielded with κ values ranging from 0.02 to 0.8 (Petters et al., 2009).

ACPD
14, 14889–14931, 2014

4.5 CCN closure tests

In this section, we compare N_{CCN} observations with corresponding values that were estimated on the basis of aerosol particle number size distributions measured in parallel and non-parallel assuming uniform chemical composition of aerosol particles. If the estimated and observed N_{CCN} agree quantitatively within the range of their uncertainty, closure is achieved. By using averaged CDF fit curve method with an assumption of uniform chemical composition, CCN size distributions were firstly calculated by multiplying the CCN efficiency spectra (3-parameter CDF fits of N_{CCN}/N_{CN}) with the total aerosol particle (CN) number size distributions measured in parallel and non-parallel. Estimated N_{CCN} were calculated by stepwise integration of the CCN size distributions from 10 to 500 nm.

4.5.1 Parallel observation (PO) closure tests

The comparison of estimated and parallelly observed N_{CCN} at five SS of 0.08 to 0.80 % is shown in Fig. 6. In this study, we named it as parallel observation (PO) closure tests. At SS > 0.23 %, a good agreement between estimated and measured N_{CCN} was obtained. The slopes are 1.04 (R^2 = 0.95) and 0.93 (R^2 = 0.97) at SS = 0.42 % and SS = 0.80 %, respectively. These slopes are close to 1.0 and the correlations are high as well, indicating that the estimation on a basis of mean CDF fit AR curve methods can estimate the observed N_{CCN} pretty well when SS is high. However, at SS of 0.08 and 0.11 %, only a reasonable correlation between estimated and measured was obtained. These slopes indicate that, despite the reasonable overall agreement, the estimation on a basis of the method underestimates about 25–30 % of the observed N_{CCN} at low SS. The reason for this disagreement and low correlation lies in that size-resolved activation ratios exhibit a larger variability at low SS than that at higher SS. Another possible reason is the decrease of MAF at low SS. Overall, in PO closure study, the averaged CDF fit method can estimate N_{CCN} well at high SS of > 0.2 % although uniform and internally mixed chemical composition throughout the size range being assumed.

ACPD
14, 14889–14931, 2014

4.5.2 Non-parallel observation (NPO) closure tests

In this study, we also estimate CCN number concentrations based on non-parallel CN size distribution measurements (12–25 June 2013) by using CDF fit curve derived from the size-resolved CCN measurements (7–21 July 2013). The comparison of estimated N_{CCN} and the non-parallel measured at three SS of 0.2, 0.5 and 0.8 % are shown in Fig. 7. A reasonable agreement between estimated and measured N_{CCN} was obtained by using CDF fit curve method. The slopes are much close to 1.0. However, only a reasonable correlation with mean R^2 of about 0.7 between estimated and measured N_{CCN} was achieved, which suggests temporal variations both in chemical composition or mixing state of aerosol particles. The lower slope at SS = 0.2 % indicates that the estimation on a basis of NPO closure underestimates about 7 % of the observed N_{CCN}. The closure is considerably improved at higher SS. Overall, the uncertainties in such NPO CCN closure study are about 30–40 %. Thus, it is important to conduct such field experiment to measure CCN under different environmental conditions. Likewise, caution needs to be exercised to use data from any experiment of short periods at a single site to do CCN parameterization for any large-scale applications. It is necessary to conduct long-term CCN measurements at more regional sites, especially those with heavy pollution of high CN.

4.6 Case study: implications of CCN activation combining chemical composition

To understand the behavior of CCN activation under different surrounding circumstance, two cases with $N_{CN} < 15\,000\,cm^{-3}$ and $> 15\,000\,cm^{-3}$ during the campaign are selected for investigation, which are defined as clean condition and polluted condition, respectively. Interestingly, bulk CCN activation exhibits completely different changes with N_{CN} from the two cases: the AR at all three SS of 0.2, 0.5 and 0.8 % increase with the increase of N_{CN} in relatively clean condition (Fig. 8a), whereas they decline with increase of N_{CN} during polluted condition (Fig. 8b). This implies totally opposite or

ACPD
14, 14889–14931, 2014

distinct mechanisms influencing the particle activation properties. To further study the impacts from chemical composition and particle size, diurnal variations of AR, derived κ_{chem} and fraction of total organic mass signal at m/z 44 (f_{44}) (Fig. 8c and d) and mass concentrations of black carbon (BC), organics, nitrate (NO_3^-), ammonium (NH_4^+), sulfate (SO_4^{2-}), chloride (Cl^-) irons etc. (Fig. 8e and f) are also plotted.

In clean days, AR shows significant diurnal variations and the changes display an apparent dependence on κ_{chem}: AR increases with the increase of κ_{chem}. This indicates the particle activation is well correlated with κ_{chem}. Because κ_{chem} is derived from chemical volume fractions and hygroscopicity parameter for the individual component, chemical composition thus plays a dominant role in the CCN activation. Actually, high correlations between bulk AR and κ_{chem} were observed when CN number concentrations are low during the campaign (Fig. 9). In these cases, organics account for relatively low amounts ($\sim 30\,\%$) of total particle mass concentrations but concentrations of soluble inorganics are high (Fig. 8e). Especially, mass concentration of nitrate is higher than organics accounting for the largest mass fraction of all compositions when κ_{chem} reaches the maximum with a mean value of 0.41. The f_{44}, which is the fraction of total organic mass signal at m/z 44, is not correlated with AR (Fig. 8c). The m/z 44 signal is due mostly to acids (Takegawa et al., 2007; Duplissy et al., 2011) or acid-derived species, such as esters, and f_{44} is closely related to the organic oxidation level (i.e., O : C ratio) (Aiken et al., 2008). Usually, the oxidized/aged acids are more hygroscopic and easily activated. Therefore, the deteriorated correlations between f_{44} and AR implied that organics in clean days are less hygroscopic during the campaign.

In addition, CN number concentrations at size range of nucleation, Aitken and accumulated mode are also shown in Fig. 8g and h for clean and polluted conditions respectively. In clean days, AR is correlated well with the changes of particle concentration at accumulated mode, suggesting aerosol particles at the size range of > 100 nm can be mostly activated under relatively uniform chemical composition. AR also shows moderate correlation with Aitken mode particles, and the correlation is not so well as the

ACPD
14, 14889–14931, 2014

accumulated mode particles, as is attributed to smaller particles with Aitken diameter of < 40 nm at the given SS (0.2–0.8 %) are difficult or cannot be activated.

During polluted events, AR shows significant diurnal variations but the changes have no apparent dependence on changes of κ_{chem} (Fig. 8d, also see Fig. 9). In contrast, variation of AR is closely related to variation of f_{44}: the AR increases with the increase of f_{44} (Fig. 8d). As stated above, the f_{44} is closely related to the organic oxidation level. Usually, the oxidized/aged acids are more hygroscopic and easily activated, suggesting the significant roles of organics contributions from oxidized or aged aerosols to CCN activity. In this case, organics account for largest amounts (with average percent of 44 %) of total particle mass concentrations (Fig. 8f). The high fraction of organics makes the derived κ_{chem} low with a mean value of 0.35. However, based on the weak correlation between AR and κ_{chem} under heavy pollutions, it cannot be inferred that AR is less dependent on or influenced by chemical composition of the particles, because the impact from organics on the particles activation is complicated (Jimenez et al., 2009). In addition, one cannot use only an empirical value (in this study we suppose $\kappa_{org} = 0.1$) to describe the particle hygroscopicity and activation properties due to the complexity of the organic aerosol fraction and its tendency to evolve with atmospheric oxidative processing and aerosol aging based on previous studies (e.g. Padró et al., 2010; Engelhart et al., 2011, 2012; Asa-Awuku et al., 2011).

Similarly, under polluted conditions, AR is more correlated with the changes of accumulated mode particles than the variations of Aitken particles. It suggests that aerosols with large particle diameter (> 100 nm) can be more easily activated, consistent with Köhler theory (Köhler, 1936). No correlation was observed between the bulk AR and particle number concentrations at Aitken mode. In the case of polluted days during the campaign, CN aerosols are mainly from biomass burning, which are usually those fine particles in nucleation or Aitken mode composed of less hygroscopic organics and thus cannot be activated to CCN. This can give a reasonable explanation of why bulk AR at the three SS shows decrease along with the increase of N_{CN} during polluted events presented in Fig. 8b. During the biomass burning events, although the total N_{CN}

ACPD
14, 14889–14931, 2014

increased, no more particles was activated to CCN, as thus lead to the decrease of the bulk AR.

5 Summary and conclusions

Atmospheric aerosol particles acting as CCN are pivotal elements of the hydrological cycle and climate change. In this study, we measured and characterized CCN in relatively clean and polluted air during the AC^{3}Exp campaign conducted at Xianghe, China during summer 2013, with the aim of understanding the CCN activation properties under high aerosol loading in the polluted regions and implying the impacts of particle size and chemical composition on CCN activation ratio to the proxy of total aerosol particles in the atmosphere.

Based on the CDF fit method, we derived that about 14–22 % of aerosol particles during the observed periods cannot be activated under typical atmospheric SS of about 0.4 %. The low MAF observed during the campaign indicates externally mixed CCN-inactive particles consisting of only non-hygroscopic species. We also found a high sensitivity of MAF dependence on SS under polluted conditions, implying that CCN activity would be changed much more evidently when changing the SS in the regions with heavy pollutions. We observed that particles with diameter of 120–160 nm were on average more hygroscopic than particles with diameter of 30–60 nm. For particles in the accumulation size range (80–180 nm), κ for polluted aerosols are about 16–35 % lower than that for clean aerosols. In contrast, for particles in the nucleation or Aitken size range (30–60 nm), κ for polluted particles is slightly higher than that for clean aerosols. The slight enhancement in hygroscopisity parameter for smaller particles during polluted events is probably because of the aerosol aging and coating process. The low R^2 for the NPO CCN closure test suggests about 30–40 % uncertainties in N_{CCN} prediction that is mainly caused by changes in particle composition. By combining analyses of chemical composition data from ACSM measurement, the relationship between bulk AR and the physical and chemical properties of the atmospheric aerosol is investigated.

ACPD
14, 14889–14931, 2014

It showed that CCN activation ratio (AR) increased with the increase of condensation nuclei (CN) number concentrations (N_{CN}) in relatively clean days. In the case, AR exhibited good correlation with κ_{chem}, which is calculated from chemical volume fractions, due to particles mainly composed of soluble inorganics. However, AR declined with increase of N_{CN} during polluted events when particles composed mostly of organics. In this case, AR is closely related to f_{44}, which is the fraction of total organic mass signal at m/z 44 and closely associated with particle organic oxidation level.

Our study implied that chemical compositions effect on aerosols hygroscopicity and CCN activation is complex but important. Especially, it has been further confirmed that CCN measurements at more locations, especially those with heavy pollutions, are necessary.

Acknowledgements. This work was funded by the National Basic Research Program of China "973" (grant no. 2013CB955801) and supported by "the Fundamental Research Funds for the Central Universities (grant no. 2013YB35)". The support of the entire AC^{3}Exp team has been much appreciated.

References

Aiken, A. C., DeCarlo, P. F., Kroll, J. H., Worsnop, D. R., Huffman, J. A., Docherty, K. S., Ulbrich, I. M., Mohr, C., Kimmel, J. R., Sueper, D., Sun, Y., Zhang, Q., Trimborn, A., Northway, M., Ziemann, P. J., Canagaratna, M. R., Onasch, T. B., Alfarra, M. R., Prevot, A. S. H., Dommen, J., Duplissy, J., Metzger, A., Baltensperger, U., and Jimenez, J. L.: O/C and OM/OC ratios of primary, secondary, and ambient organic aerosols with high-resolution time-of-flight aerosol mass spectrometry, Environ. Sci. Technol., 42, 4478–4485, 2008.

Albrecht, B. A.: Aerosols, clouds and microphysics, Science, 245, 1227–1230, 1989.

Alfarra, M. R., Coe, H., Allan, J. D., Bower, K. N., Boudries, H., Canagaratna, M. R., Jimenez, J. L., Jayne, J. T., Garforth, A. A., Li, S.-M., and Worsnop, D. R.: Characterization of urban and rural organic particulate in the Lower Fraser Valley using two Aerodyne Aerosol Mass Spectrometers, Atmos. Environ., 38, 5745–5758, 2004.

ACPD
14, 14889–14931, 2014

Andreae, M. O. and Rosenfeld, D.: Aerosol-cloudprecipitation interactions. Part 1. The nature and sources of cloud-active aerosols, Earth. Sci. Rev., 89, 13–41, doi:10.1016/j.earscirev.2008.03.001, 2008.

Anttila, T. and Kerminen, V.-M.: On the contribution of Aitken mode particles to cloud droplet populations at continental background areas – a parametric sensitivity study, Atmos. Chem. Phys., 7, 4625–4637, doi:10.5194/acp-7-4625-2007, 2007.

Asa-Awuku, A., Moore, R. H., Nenes, A., Bahreini, R., Holloway, J. S., Brock, C. A., Middlebrook, A. M., Ryerson, T., Jimenez, J., DeCarlo, P., Hecobian, A., Weber, R., Stickel, R., Tanner, D. J., and Huey, L. G.: Airborne cloud condensation nuclei measurements during the 2006 Texas Air Quality Study, J. Geophys. Res., 116, D11201, doi:10.1029/2010JD014874, 2011.

Bougiatioti, A., Fountoukis, C., Kalivitis, N., Pandis, S. N., Nenes, A., and Mihalopoulos, N.: Cloud condensation nuclei measurements in the marine boundary layer of the Eastern Mediterranean: CCN closure and droplet growth kinetics, Atmos. Chem. Phys., 9, 7053–7066, doi:10.5194/acp-9-7053-2009, 2009.

Bougiatioti, A., Nenes, A., Fountoukis, C., Kalivitis, N., Pandis, S. N., and Mihalopoulos, N.: Size-resolved CCN distributions and activation kinetics of aged continental and marine aerosol, Atmos. Chem. Phys., 11, 8791–8808, doi:10.5194/acp-11-8791-2011, 2011.

Chuang, P. Y., Collins, D. R., Pawlowska, H., Snider, J. R., Jonsson, H. H., Brenguier, J. L., Flagan, R. C., and Seinfeld, J. H.: CCN measurements during ACE-2 and their relationship to cloud microphysical properties, Tellus B, 52, 843–867, 2000.

Clarke, A., McNaughton, C., Kasputin, V. N., Shinozuka, Y., Howell, S., Dibb, J., Zhou, J., Anderson, B., Brekhovskikh, V., Turner, H., and Pinkerton, M.: Biomass burning and pollution aerosol over North America: organic components and their influence on spectral optical properties and humidification response, J. Geophys. Res., 112, D12S18, doi:10.1029/2006JD007777, 2007.

Deng, Z. Z., Zhao, C. S., Ma, N., Liu, P. F., Ran, L., Xu, W. Y., Chen, J., Liang, Z., Liang, S., Huang, M. Y., Ma, X. C., Zhang, Q., Quan, J. N., Yan, P., Henning, S., Mildenberger, K., Sommerhage, E., Schäfer, M., Stratmann, F., and Wiedensohler, A.: Size-resolved and bulk activation properties of aerosols in the North China Plain, Atmos. Chem. Phys., 11, 3835–3846, doi:10.5194/acp-11-3835-2011, 2011.

Deng, Z. Z., Zhao, C. S., Ma, N., Ran, L., Zhou, G. Q., Lu, D. R., and Zhou, X. J.: An examination of parameterizations for the CCN number concentration based on in situ measurements of

ACPD
14, 14889–14931, 2014

aerosol activation properties in the North China Plain, Atmos. Chem. Phys., 13, 6227–6237, doi:10.5194/acp-13-6227-2013, 2013.
Duplissy, J., DeCarlo, P. F., Dommen, J., Alfarra, M. R., Metzger, A., Barmpadimos, I., Prevot, A. S. H., Weingartner, E., Tritscher, T., Gysel, M., Aiken, A. C., Jimenez, J. L., Canagaratna, M. R., Worsnop, D. R., Collins, D. R., Tomlinson, J., and Baltensperger, U.: Relating hygroscopicity and composition of organic aerosol particulate matter, Atmos. Chem. Phys., 11, 1155–1165, doi:10.5194/acp-11-1155-2011, 2011.
Dusek, U., Covert, D. S., Wiedensohler, A., Neususs, C., Weise, D., and Cantrell, W.: Cloud condensation nuclei spectra derived from size distributions and hygroscopic properties of the aerosol in coastal south-west Portugal during ACE-2, Tellus B, 55, 35–53, 2003.
Dusek, U., Frank, G. P., Hildebrandt, L., Curtius, J., Schneider, J., Walter, S., Chand, D., Drewnick, F., Hings, S., Jung, D., Borrmann, S., and Andreae, M. O.: Size matters more than chemistry for cloud-nucleating ability of aerosol particles, Science, 312, 1375–1378, 2006a.
Dusek, U., Reischl, G. P., and Hitzenberger, R.: CCN activation of pure and coated carbon black particles, Environ. Sci. Technol., 40, 1223–1230, 2006b.
Engelhart, G. J., Moore, R. H., Nenes, A., and Pandis, S. N.: Cloud condensation nuclei activity of isoprene secondary organic aerosol, J. Geophys. Res., 116, D02207, doi:10.1029/2010JD014706, 2011.
Engelhart, G. J., Hennigan, C. J., Miracolo, M. A., Robinson, A. L., and Pandis, S. N.: Cloud condensation nuclei activity of fresh primary and aged biomass burning aerosol, Atmos. Chem. Phys., 12, 7285–7293, doi:10.5194/acp-12-7285-2012, 2012.
Ervens, B., Feingold, G., and Kreidenweis, S.: Influence of watersoluble organic carbon on cloud drop number concentration, J. Geophys. Res., 110, D18211, doi:10.1029/2004JD005634, 2005.
Feingold, G.: Modeling of the first indirect effect: analysis of measurement requirements, Geophys. Res. Lett., 30, doi:10.1029/2003GL017967, 2003.
Gasparini, R., Collins, D. R., Andrews, E., Sheridan, P. J., Ogren, J. A., and Hudson, J. G.: Coupling aerosol size distributions and size-resolved hygroscopicity to predict humidity-dependent optical properties and cloud condensation nuclei spectra, J. Geophys. Res., 111, D05S13, doi:10.1029/2005JD006092, 2006.
Gunthe, S. S., King, S. M., Rose, D., Chen, Q., Roldin, P., Farmer, D. K., Jimenez, J. L., Artaxo, P., Andreae, M. O., Martin, S. T., and Pöschl, U.: Cloud condensation nuclei in

ACPD
14, 14889–14931, 2014

pristine tropical rainforest air of Amazonia: size-resolved measurements and modeling of atmospheric aerosol composition and CCN activity, Atmos. Chem. Phys., 9, 7551–7575, doi:10.5194/acp-9-7551-2009, 2009.

Hartz, K. E. H., Tischuk, J. E., Chan, M. N., Chan, C. K., Donahue, N. M., and Pandis, S. N.: Cloud condensation nuclei activation of limited solubility organic aerosol, Atmos. Environ., 40, 605–617, 2006.

Hudson, J.: Variability of the relationship between particle size and cloud-nucleating ability, Geophys. Res. Lett., 34, L08801, doi:10.1029/2006GL028850, 2007.

IPCC: Climate Change 2007: Scientific Basis, Fourth Assessment Of The Inter-Governmental Panel on Climate Change, Cambridge Univ. Press, New York, 2007.

IPCC: Climate change 2013: Scientific Basis, Fifth Assessment of the Inter-Governmental Panel on Climate Change, Cambridge Univ. Press, New York, 2013.

Jimenez, J. L., Canagaratna, M. R., Donahue, N. M., Prevot, A. S. H., Zhang, Q., Kroll, J. H., DeCarlo, P. F., Allan, J. D., Coe, H., Ng, N. L., Aiken, A. C., Docherty, K. S., Ulbrich, I. M., Grieshop, A. P., Robinson, A. L., Duplissy, J., Smith, J. D., Wilson, K. R., Lanz, V. A., Hueglin, C., Sun, Y. L., Tian, J., Laaksonen, A., Raatikainen, T., Rautiainen, J., Vaattovaara, P., Ehn, M., Kulmala, M., Tomlinson, J. M., Collins, D. R., Cubison, M. J., Dunlea, E. J., Huffman, J. A., Onasch, T. B., Alfarra, M. R., Williams, P. I., Bower, K., Kondo, Y., Schneider, J., Drewnick, F., Borrmann, S., Weimer, S., Demerjian, K., Salcedo, D., Cottrell, L., Griffin, R., Takami, A., Miyoshi, T., Hatakeyama, S., Shimono, A., Sun, J. Y., Zhang, Y. M., Dzepina, K., Kimmel, J. R., Sueper, D., Jayne, J. T., Herndon, S. C., Trimborn, A. M., Williams, L. R., Wood, E. C., Middlebrook, A. M., Kolb, C. E., Baltensperger, U., and Worsnop, D. R.: Evolution of organic aerosols in the atmosphere, Science, 326, 1525–1529, 2009.

Köhler, H.: The nucleus in and growth of hygroscopic droplets, T. Faraday Soc., 32, 1152–1161, doi:10.1039/TF9363201152, 1936.

Kreidenweis, S. M., Petters, M. D., and DeMott, P. J.: Single-parameter estimates of aerosol water content,Environ. Res. Lett., 3, 035002 doi:10.1088/1748-9326/3/3/035002, 2008.

Kuwata, M., Kondo, Y., Mochida, M., Takegawa, N., and Kawamura, K.: Dependence of CCN activity of less volatile particles on the amount of coating observed in Tokyo, J. Geophys. Res., 112, D11207, doi:10.1029/2006JD007758, 2007.

ACPD
14, 14889–14931, 2014

Kuwata, M., Kondo, Y., Miyazaki, Y., Komazaki, Y., Kim, J. H., Yum, S. S., Tanimoto, H., and Matsueda, H.: Cloud condensation nuclei activity at Jeju Island, Korea in spring 2005, Atmos. Chem. Phys., 8, 2933–2948, doi:10.5194/acp-8-2933-2008, 2008.

Lance, S., Medina, J., Smith, J., and Nenes, A.: Mapping the operation of the DMT continuous flow CCN counter, Aerosol Sci. Tech., 40, 242–254, 2006.

Lathem, T. L., Beyersdorf, A. J., Thornhill, K. L., Winstead, E. L., Cubison, M. J., Hecobian, A., Jimenez, J. L., Weber, R. J., Anderson, B. E., and Nenes, A.: Analysis of CCN activity of Arctic aerosol and Canadian biomass burning during summer 2008, Atmos. Chem. Phys., 13, 2735–2756, doi:10.5194/acp-13-2735-2013, 2013.

Lau, K. M., Ramahathan, V., Wu, G., Li, Z., Tsay, S. C., Hsu, C., Sikka, R., Holben, B., Lu, D., Tartari, G., Chin, M., Koudelova, P., Chen, H., Ma, Y., Huang, J., Taniguchi, K., and Zhang, R.: The joint aerosol monsoon experiment: a new challenge for monsoon climate research, B. Am. Meteorol. Soc., 89, 369–383, doi:10.1175/BAMS-89-3-369, 2008.

Lee, S. H., Murphy, D. M., Thomson, D. S., and Middlebrook, A. M.: Nitrate and oxidized organic ions in single particle mass spectra during the 1999 Atlanta Supersite Project, J. Geophys. Res., 108, 8417, doi:10.1029/2001JD001455, 2003.

Lee, Y. S., Collins, D. R., Li, R. J., Bowman, K. P., and Feingold, G.: Expected impact of an aged biomass burning aerosol on cloud condensation nuclei and cloud droplet concentrations, J. Geophys. Res., 111, D22204, doi:10.1029/2005JD006464, 2006.

Leng, C., Cheng, T., Chen, J., Zhang, R., Tao, J., Huang, G., Zha, S., Zhang, M., Fang, W., Li, X., and Li, L.: Measurements of surface cloud condensation nuclei and aerosol activity in downtown Shanghai, Atmos. Environ., 69, 354–361, 2013.

Li, Z., Chen, H., Cribb, M., Dickerson, R. E., Holben, B., Li, C., Lu, D., Luo, Y., Maring, H., Shi, G., Tsay, S.-C., Wang, P., Wang, Y., Xia, X., Zheng, Y., Yuan, T., and Zhao, F.: Preface to special section on East Asian Studies of Tropospheric Aerosols: an International Regional Experiment (EASTAIRE), J. Geophys. Res., 112, D22S00, doi:10.1029/2007JD008853, 2007a.

Li, Z., Xia, X., Cribb, M., Mi, W., Holben, B., Wang, P., Chen, H., Tsay, S- C., Eck, T. F., Zhao, F., Dutton, E. G., and Dickerson, R. E.: Aerosol optical properties and their radiative effects in northern China, J. Geophys. Res., 112, D22S01, doi:10.1029/2006JD007382, 2007b.

Li, Z., Li, C., Chen, H., Tsay, S.-C., Holben, B., Huang, J., Li, B., Maring, H., Qian, Y., Shi, G., Xia, X., Yin, Y., Zheng, Y., and Zhuang, G.: East Asian studies of tropospheric aerosols and impact on regional climate (EAST-AIRC): an overview, J. Geophys. Res., 116, D00K34, doi:10.1029/2010JD015257, 2011.

ACPD
14, 14889–14931, 2014

Liu, J., Zheng, Y., Li, Z., and Cribb, M.: Analysis of cloud condensation nuclei properties at a polluted site in southeastern China during the AMF-China Campaign, J. Geophys. Res., 116, D00K35, doi:10.1029/2011JD016395, 2011.

Ma, Y., Brooks, S. D., Vidaurre, G., Khalizov, A. F., Wang, L.: Rapid modification of cloud-nucleating ability of aerosols by biogenic emissions, Geophys. Res. Lett. 40, 6293–6297, doi:10.1002/2013GL057895, 2013.

Mei, F., Setyan, A., Zhang, Q., and Wang, J.: CCN activity of organic aerosols observed downwind of urban emissions during CARES, Atmos. Chem. Phys., 13, 12155–12169, doi:10.5194/acp-13-12155-2013, 2013.

Mikhailov, E., Vlasenko, S., Martin, S. T., Koop, T., and Pöschl, U.: Amorphous and crystalline aerosol particles interacting with water vapor: conceptual framework and experimental evidence for restructuring, phase transitions and kinetic limitations, Atmos. Chem. Phys., 9, 9491–9522, doi:10.5194/acp-9-9491-2009, 2009.

Mircea, M., Facchini, M. C., Decesari, S., Cavalli, F., Emblico, L., Fuzzi, S., Vestin, A., Rissler, J., Swietlicki, E., Frank, G., Andreae, M. O., Maenhaut, W., Rudich, Y., and Artaxo, P.: Importance of the organic aerosol fraction for modeling aerosol hygroscopic growth and activation: a case study in the Amazon Basin, Atmos. Chem. Phys., 5, 3111–3126, doi:10.5194/acp-5-3111-2005, 2005.

Niedermeier, D., Wex, H., Voigtländer, J., Stratmann, F., Brüggemann, E., Kiselev, A., Henk, H., and Heintzenberg, J.: LACIS-measurements and parameterization of sea-salt particle hygroscopic growth and activation, Atmos. Chem. Phys., 8, 579–590, doi:10.5194/acp-8-579-2008, 2008.

Ng, N. L., Herndon, S. C., Trimborn, A., Canagaratna, M. R., Croteau, P. L., Onasch, T. B., Sueper, D.,Worsnop, D. R., Zhang, Q., Sun, Y. L., and Jayne, J. T.: An Aerosol Chemical Speciation Monitor (ACSM) for routine monitoring of the composition and mass concentrations of ambient aerosol, Aerosol Sci. Tech., 45, 770–784, 2011.

Padró, L. T., Tkacik, D., Lathem, T. L., Hennigan, C. J., Sullivan, A. P., Weber, R. J., Huey, L. G., and Nenes, A.: Investigation of cloud condensation nuclei properties and droplet growth kinetics of the water-soluble aerosol fraction in Mexico City, J. Geophys. Res., 115, D09204, doi:10.1029/2009JD013195, 2010.

Paramonov, M., Aalto, P. P., Asmi, A., Prisle, N., Kerminen, V.-M., Kulmala, M., and Petäjä, T.: The analysis of size-segregated cloud condensation nuclei counter (CCNC) data and its

ACPD
14, 14889–14931, 2014

implications for aerosol-cloud interactions, Atmos. Chem. Phys. Discuss., 13, 9681–9731, doi:10.5194/acpd-13-9681-2013, 2013.
Petters, M. D. and Kreidenweis, S. M.: A single parameter representation of hygroscopic growth and cloud condensation nucleus activity, Atmos. Chem. Phys., 7, 1961–1971, doi:10.5194/acp-7-1961-2007, 2007.
Petters, M. D., Carrico, C. M., Kreidenweis, S. M., Prenni, A. J., DeMott, P. J., Collett, J. L., and Moosmüller, H.: Cloud condensation nucleation activity of biomass burning aerosol, J. Geophys. Res., 114, D22205, doi:10.1029/2009JD012353, 2009.
Pringle, K. J., Tost, H., Pozzer, A., Pöschl, U., and Lelieveld, J.: Global distribution of the effective aerosol hygroscopicity parameter for CCN activation, Atmos. Chem. Phys., 10, 5241–5255, doi:10.5194/acp-10-5241-2010, 2010.
Quinn, P. K., Bates, T. S., Coffman, D. J., and Covert, D. S.: Influence of particle size and chemistry on the cloud nucleating properties of aerosols, Atmos. Chem. Phys., 8, 1029–1042, doi:10.5194/acp-8-1029-2008, 2008.
Raymond, T. M. and Pandis, S. N.: Cloud activation of single component organic aerosol particles, J. Geophys. Res., 107, 4787, doi:10.1029/2002JD002159, 2002.
Rissler, J., Swietlicki, E., Zhou, J., Roberts, G., Andreae, M. O., Gatti, L. V., and Artaxo, P.: Physical properties of the sub-micrometer aerosol over the Amazon rain forest during the wet-to-dry season transition – comparison of modeled and measured CCN concentrations, Atmos. Chem. Phys., 4, 2119–2143, doi:10.5194/acp-4-2119-2004, 2004.
Roberts, G. C., Artaxo, P., Zhou, J. C., Swietlicki, E., and Andreae, M. O.: Sensitivity of CCN spectra on chemical and physical properties of aerosol: a case study from the Amazon Basin, J. Geophys. Res., 107, 8070, doi:10.1029/2001JD000583, 2002.
Rose, D., Nowak, A., Achtert, P., Wiedensohler, A., Hu, M., Shao, M., Zhang, Y., Andreae, M. O., and Pöschl, U.: Cloud condensation nuclei in polluted air and biomass burning smoke near the mega-city Guangzhou, China – Part 1: Size-resolved measurements and implications for the modeling of aerosol particle hygroscopicity and CCN activity, Atmos. Chem. Phys., 10, 3365–3383, doi:10.5194/acp-10-3365-2010, 2010.
Rose, D., Gunthe, S. S., Su, H., Garland, R. M., Yang, H., Berghof, M., Cheng, Y. F., Wehner, B., Achtert, P., Nowak, A., Wiedensohler, A., Takegawa, N., Kondo, Y., Hu, M., Zhang, Y., Andreae, M. O., and Pöschl, U.: Cloud condensation nuclei in polluted air and biomass burning smoke near the mega-city Guangzhou, China – Part 2: Size-resolved aerosol chemical

ACPD
14, 14889–14931, 2014

composition, diurnal cycles, and externally mixed weakly CCN-active soot particles, Atmos. Chem. Phys., 11, 2817–2836, doi:10.5194/acp-11-2817-2011, 2011.
Rose, D., Gunthe, S. S., Mikhailov, E., Frank, G. P., Dusek, U., Andreae, M. O., and Pöschl, U.: Calibration and measurement uncertainties of a continuous-flow cloud condensation nuclei counter (DMT-CCNC): CCN activation of ammonium sulfate and sodium chloride aerosol particles in theory and experiment, Atmos. Chem. Phys., 8, 1153–1179, doi:10.5194/acp-8-1153-2008, 2008.
Rosenfeld, D., Dai, J., Yu, X., Yao, Z., Xu, X., Yang, X., and Du, C.: Inverse relations between amounts of air pollution and orographic precipitation, Science, 315, 1396–1398, doi:10.1126/science.1137949, 2007.
Salcedo, D., Onasch, T. B., Dzepina, K., Canagaratna, M. R., Zhang, Q., Huffman, J. A., DeCarlo, P. F., Jayne, J. T., Mortimer, P., Worsnop, D. R., Kolb, C. E., Johnson, K. S., Zuberi, B., Marr, L. C., Volkamer, R., Molina, L. T., Molina, M. J., Cardenas, B., Bernabé, R. M., Márquez, C., Gaffney, J. S., Marley, N. A., Laskin, A., Shutthanandan, V., Xie, Y., Brune, W., Lesher, R., Shirley, T., and Jimenez, J. L.: Characterization of ambient aerosols in Mexico City during the MCMA-2003 campaign with Aerosol Mass Spectrometry: results from the CENICA Supersite, Atmos. Chem. Phys., 6, 925–946, doi:10.5194/acp-6-925-2006, 2006.
Sotiropoulou, R. E. P., Nenes, A., Adams, P. J., and Seinfeld, J. H.: Cloud condensation nuclei prediction error from application of Köhler theory: importance for the aerosol indirect effect, J. Geophys. Res., 112, D12202, doi:10.1029/2006JD007834, 2007.
Streets, D. G., Yu, C., Wu, Y., Chin, M., Zhao, Z., Hayasaka, T., and Shi, G.: Aerosol trends over China, 1980–2000, Atmos. Res., 88, 174–182, doi:10.1016/j.atmosres.2007.10.016, 2008.
Stroud, C. A., Nenes, A., Jimenez, J. L., DeCarlo, P., Huffman, J. A., Bruintjes, R., Nemitz, E., Delia, A. E., Toohey, D. W., Guenther, A. B., and Nandi, S.: Cloud activating properties of aerosol observed during CELTIC, J. Atmos. Sci., 64, 441–459, 2007.
Sun, Y., Wang, Z., Dong, H., Yang, T., Li, J., Pan, X., Chen, P., and Jayne, J. T.: Characterization of summer organic and inorganic aerosols in Beijing, China with an aerosol chemical speciation monitor, Atmos. Environ., 51, 250–259, doi:10.1016/j.atmosenv.2012.01.013, 2012.
Takegawa, N., Miyakawa, T., Kawamura, K., and Kondo, Y.: Contribution of selected di-carboxylic and omega-oxocarboxylic acids in ambient aerosol to the m/z 44 signal of an aerodyne aerosol mass spectrometer, Aerosol Sci. Tech., 41, 418–437, doi:10.1080/02786820701203215, 2007.

ACPD
14, 14889–14931, 2014

Turpin, B. J. and Lim, H. J.: Species contributions to $PM_{2.5}$ mass concentrations: revisiting common assumptions for estimating organic mass, Aerosol Sci. Tech., 35, 602–610, 2001.
Twomey, S.: Pollution and planetary albedo, Atmos. Environ., 8, 1251–1256, 1974.
Twomey, S.: The influence of pollution on the shortwave albedo of clouds, J. Atmos. Sci., 34, 1149–1152, doi:10.1175/1520-0469(1977)034<1149:TIOPOT>2.0.CO;2, 1977.
VanReken, T. M., Rissman, T. A., Roberts, G. C., Varutbangkul, V., Jonsson, H. H., Flagan, R. C., and Seinfeld, J. H.: Toward aerosol/cloud condensation nuclei (CCN) closure during CRYSTAL-FACE, J. Geophys. Res., 108, 4633, doi:10.1029/2003JD003582, 2003.
VanReken, T. M., Ng, N. L., Flagan, R. C., and Seinfeld, J. H.: Cloud condensation nucleus activation properties of biogenic secondary organic aerosol, J. Geophys. Res., 110, D07206, doi:10.1029/2004JD005465, 2005.
Varutbangkul, V., Brechtel, F. J., Bahreini, R., Ng, N. L., Keywood, M. D., Kroll, J. H., Flagan, R. C., Seinfeld, J. H., Lee, A., and Goldstein, A. H.: Hygroscopicity of secondary organic aerosols formed by oxidation of cycloalkenes, monoterpenes, sesquiterpenes, and related compounds, Atmos. Chem. Phys., 6, 2367–2388, doi:10.5194/acp-6-2367-2006, 2006.
Xia, X., Li, Z., Holben, B., Wang, P., Eck, T., Chen, H., Cribb, M., and Zhao, Y.: Aerosol optical properties and radiative effects in the Yangtze Delta region of China, J. Geophys. Res., 112, D22S12, doi:10.1029/2007JD008859, 2007.
Xin, J., Wang, Y., Li, Z., Wang, P., Hao, W., Nordgren, B. L., Wang, S., Liu, G., Wang, L., Wen, T., Sun, Y., and Hu, B.: AOD and Angstrom exponent of aerosols observed by the Chinese Sun Hazemeter Network from August 2004 to September 2005, J. Geophys. Res., 112, D05203, doi:10.1029/2006JD007075, 2007.
Xu, Q.: Abrupt change of the mid-summer climate in central east China by the influence of atmospheric pollution, Atmos. Environ., 35, 5029–5040, doi:10.1016/S1352-2310(01)00315-6, 2001.
Yue, D. L., Hu, M., Zhang, R. J., Wu, Z. J., Su, H., Wang, Z. B., Peng, J. F., He, L. Y., Huang, X. F., Gong, Y. G., and Wiedensohler, A.: Potential contribution of new particle formation to cloud condensation nuclei in Beijing, Atmos. Environ., 45, 6070–6077, 2011.
Yum, S. S., Roberts, G., Kim, J. H., Song, K., and Kim, D.: Submicron aerosol size distributions and cloud condensation nuclei concentrations measured at Gosan, Korea, during the Atmospheric Brown Clouds–East Asian Regional Experiment 2005, J. Geophys. Res., 112, D22S32, doi:10.1029/2006JD008212, 2007.

ACPD
14, 14889–14931, 2014

Zhang, Q., Stanier, C. O., Canagaratna, M. C., Jayne, J. T., Worsnop, D. R., Pandis, S. N., and Jimenez, J. L.: Insights into the chemistry of new particle formation and growth events in Pittsburgh based on aerosol mass spectrometry, Environ. Sci. Technol., 38, 4797–4809, 2004.

Zhang, Q., Meng, J., Quan, J., Gao, Y., Zhao, D., Chen, P., and He, H.: Impact of aerosol composition on cloud condensation nuclei activity, Atmos. Chem. Phys., 12, 3783–3790, doi:10.5194/acp-12-3783-2012, 2012.

Zhang, R., Khalizov, A. F., Pagels, J., Zhang, D., Xue, H., and McMurry, P. H.: Variability in morphology, hygroscopic and optical properties of soot aerosols during internal mixing in the atmosphere, P. Natl. Acad. Sci. USA, 105, 10291–10296, 2008.

ACPD
14, 14889–14931, 2014

Table 1. Characteristic of spectra Basic spectral parameters for polluted and background aerosols during the campaign for different super saturation. Quantities are midpoint activation diameters (D_a, D_{cut}), maximum activated fractions (MAF), CDF standard deviations (σ), heterogeneity parameters (σ/D_a), hygroscopicity parameters (κ_a, κ_{cut}).

SS	D_a_POL	D_{cut}_POL	MAF_POL	σ_POL	σ/D_a_POL	κ_a_POL	κ_{cut}_POL	D_a_BG	D_{cut}_BG	MAF_BG	σ_BG	σ/D_a_BG	κ_a_BG	κ_{cut}_BG
0.08 %	175.37	168.60	0.49	41.49	0.24	0.40	0.53	150.11	156.50	0.79	39.67	0.26	0.64	0.67
0.11 %	142.97	144.30	0.53	33.68	0.24	0.39	0.48	125.75	129.30	0.82	30.82	0.25	0.57	0.63
0.23 %	87.16	95.30	0.67	22.48	0.26	0.39	0.44	79.69	84.60	0.86	16.69	0.21	0.52	0.53
0.42 %	55.99	55.10	0.78	11.96	0.21	0.43	0.52	54.39	54.40	0.86	10.82	0.20	0.47	0.51
0.80 %	37.54	41.80	0.81	7.32	0.19	0.40	0.39	37.91	40.50	0.86	8.63	0.23	0.39	0.38

ACPD
14, 14889–14931, 2014

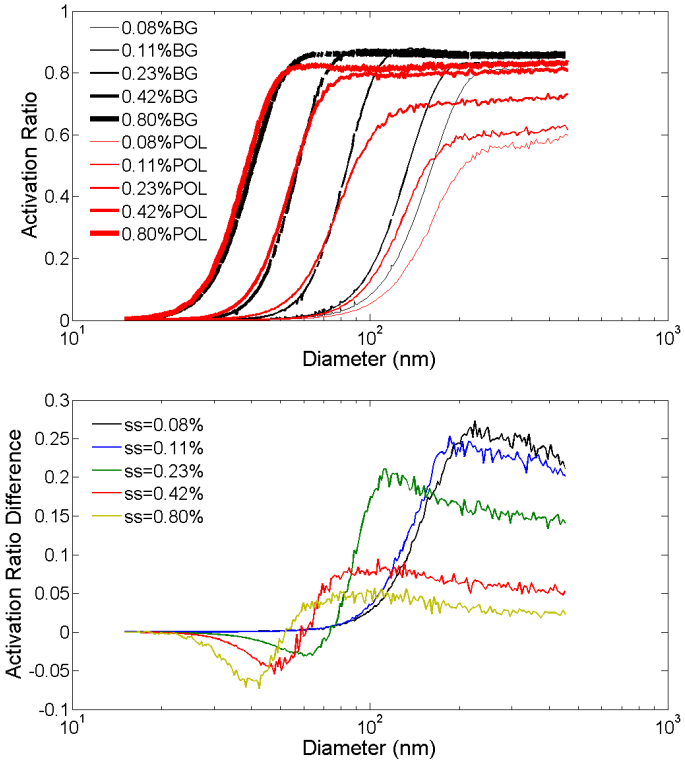

Figure 1. Averaged measured CCN efficiency spectra (top) by the 3-parameter CDF fit at SS of 0.08, 0.11, 0.23, 0.42 and 0.80 % and differences of activation ratios (bottom) between polluted and background conditions during the size-resolved CCN measurements period.

ACPD
14, 14889–14931, 2014

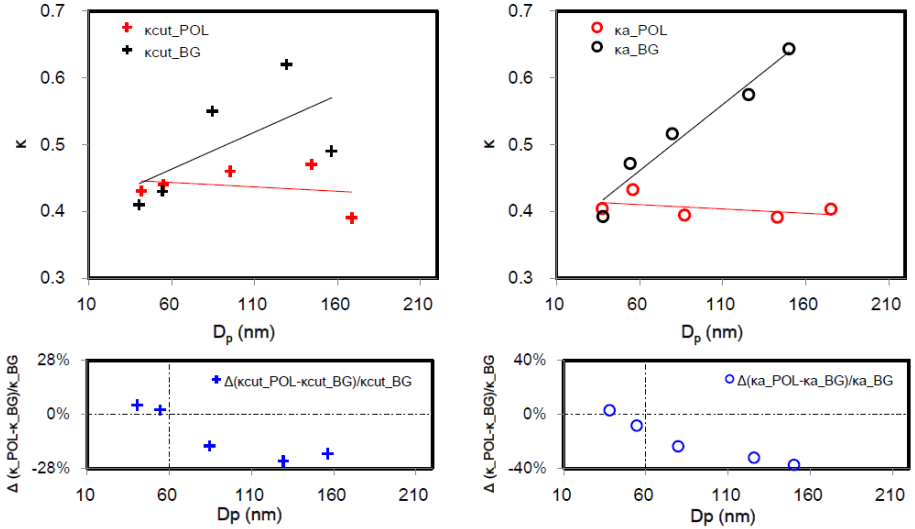

Figure 2. Characteristics of hygroscopicity parameters, κ_{cut} (upper left) and κ_a (upper right) against the particle diameters for polluted and background conditions and changes of κ_{cut} (below, left) and κ_a (below, right) due to the pollutions at each particle diameter.

ACPD
14, 14889–14931, 2014

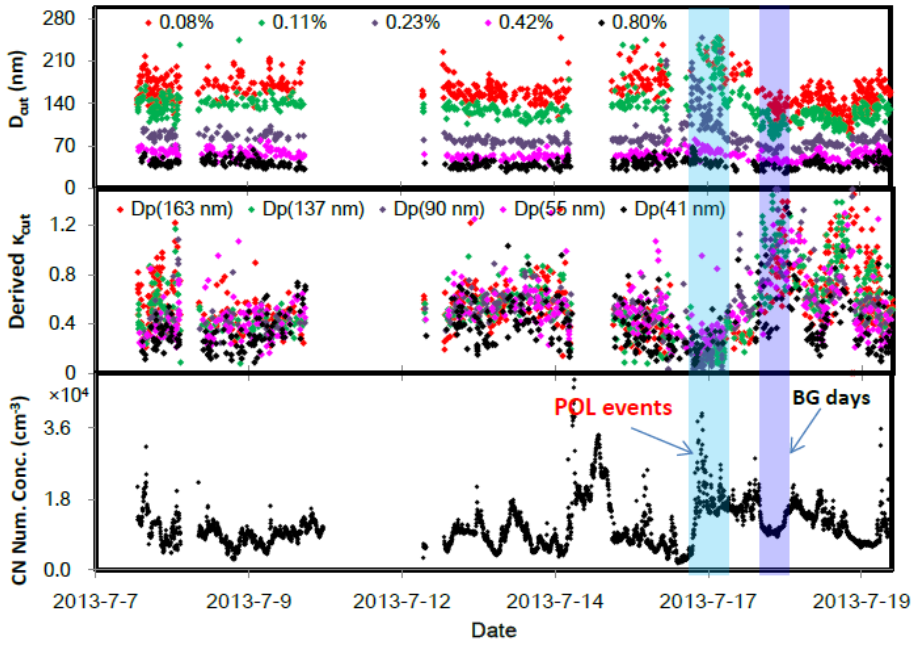

Figure 3. Time series of CN number concentrations, D_{cut} and derived κ_{cut} at five SS of 0.08–0.80 % during the size-resolved CCN measurements period.

ACPD
14, 14889–14931, 2014

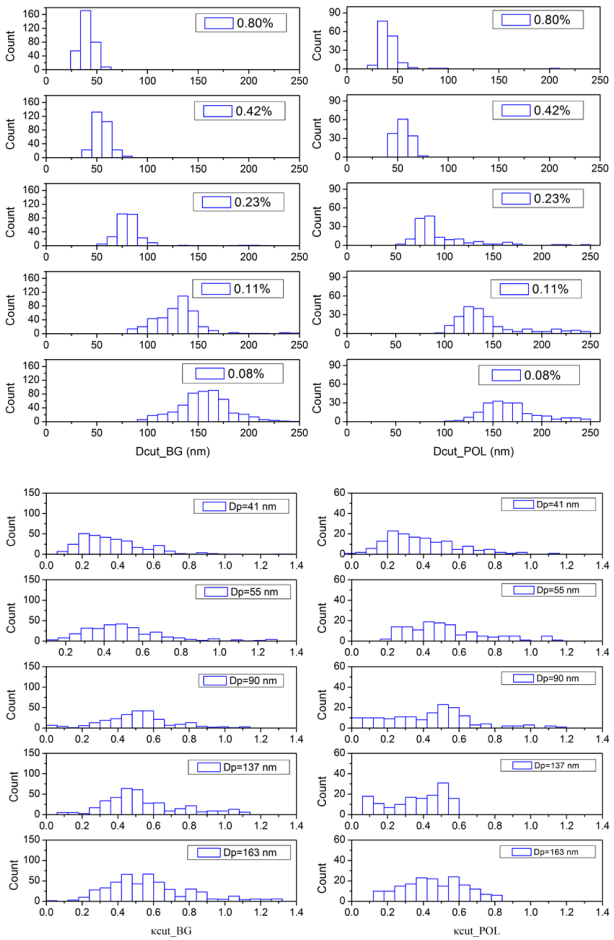

Figure 4. Probability distribution (PDF) of D_{cut} and κ_{cut} under background and polluted conditions at five SS of 0.08–0.80 % during the size-resolved CCN measurements period.

ACPD
14, 14889–14931, 2014

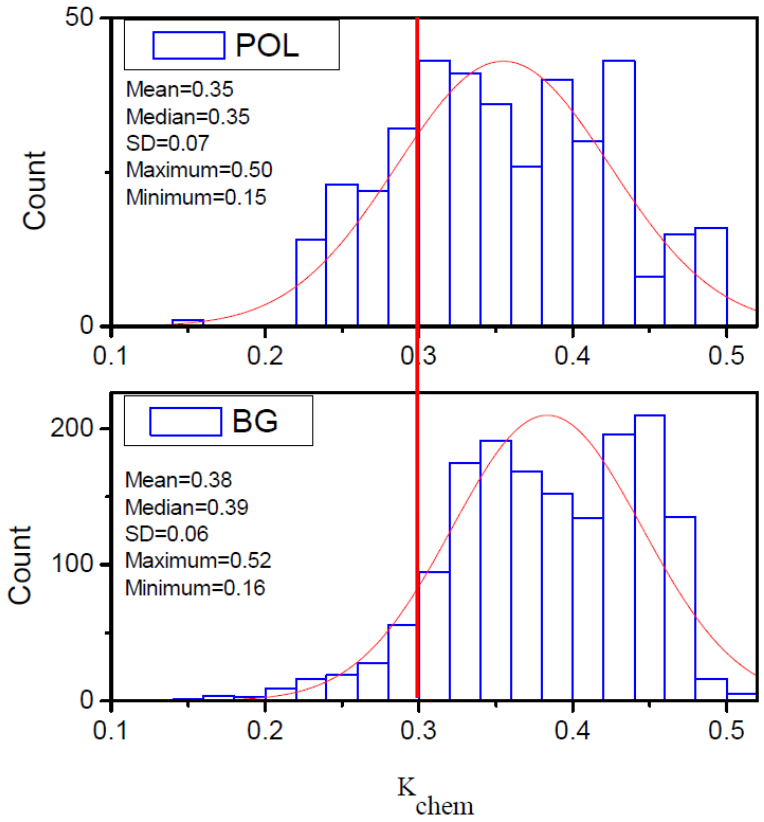

Figure 5. PDF of derived κ_{chem} under background and polluted conditions during the campaign (30 May–30 June 2013).

ACPD
14, 14889–14931, 2014

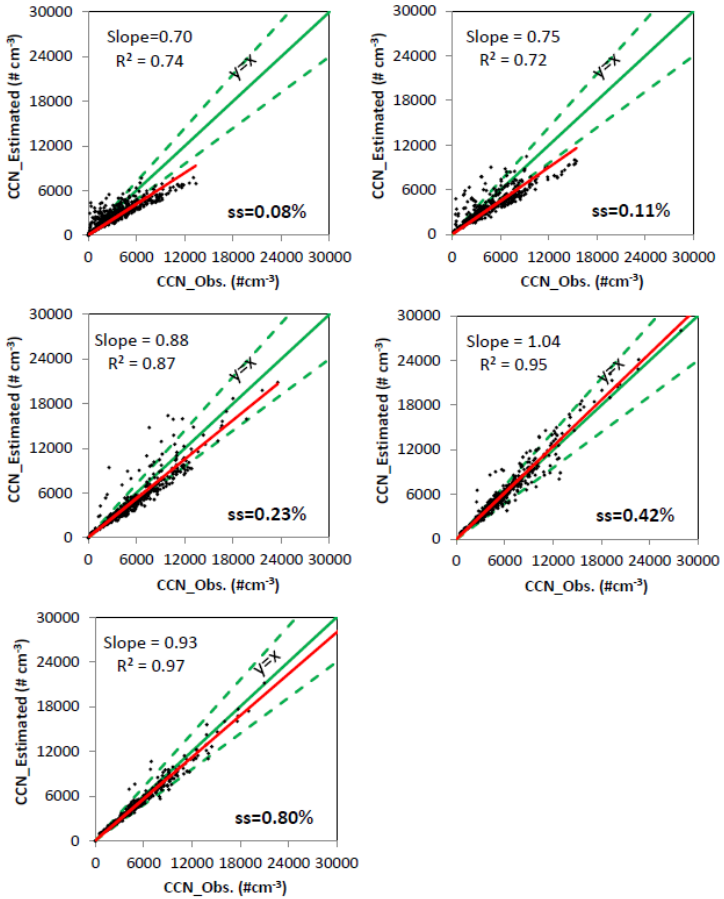

Figure 6. Estimated N_{CCN} plotted against the observed N_{CCN} in parallel observation (PO) closure test. The green solid line is the 1 : 1 line, and the dashed green lines indicate the band of about ±30 % deviation of N_{CCN}-estimated from N_{CCN}-observed.

ACPD
14, 14889–14931, 2014

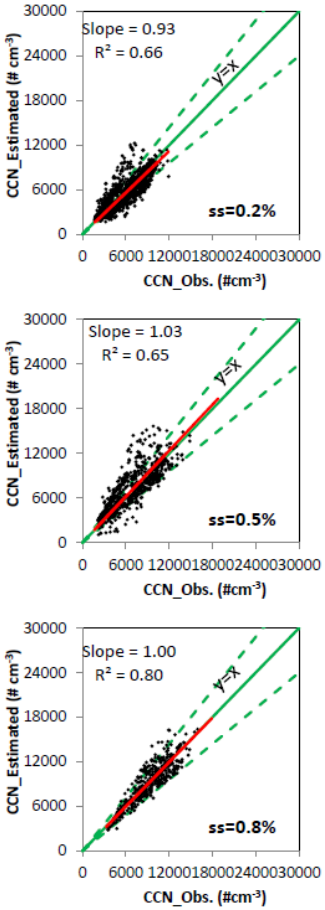

Figure 7. Estimated N_{CCN} plotted against the observed N_{CCN} in Non-parallel observation (NPO) closure test. The green solid line is the 1 : 1 line, and the dashed green lines indicate the band of about ±30 % deviation of N_{CCN}-estimated from N_{CCN}-observed.

ACPD
14, 14889–14931, 2014

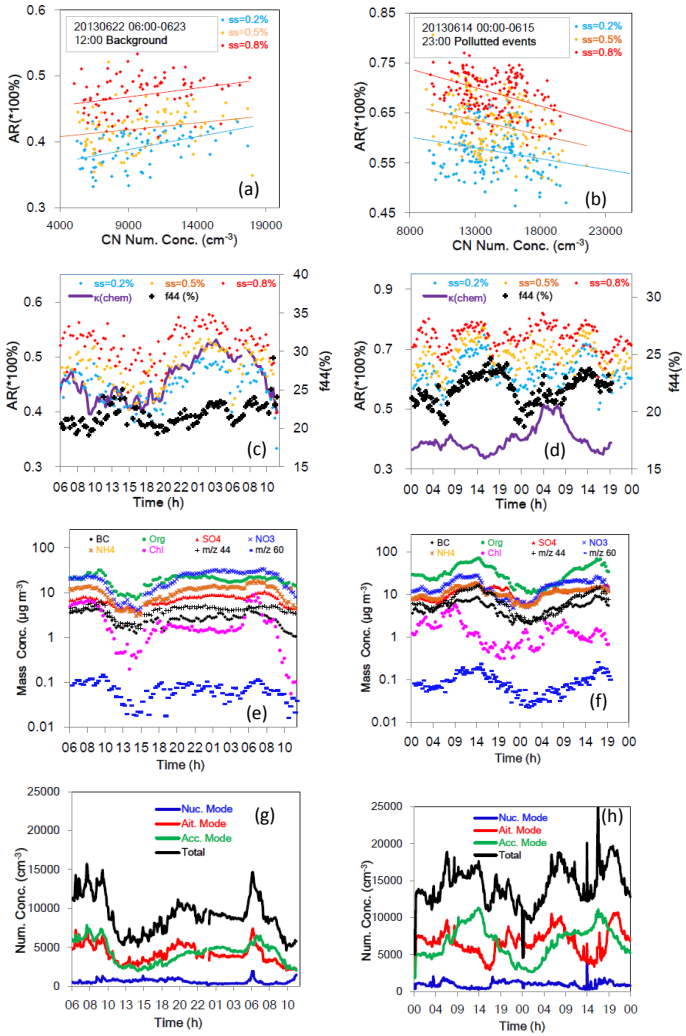

ACPD
14, 14889–14931, 2014

Aerosol hygroscopicity and CCN activity from field measurements

F. Zhang et al.

Figure 8. Two selected cases of background conditions (22–23 June 2013) with N_{CN} of < 15 000 cm^{-3} (left) and polluted events (14–15 June 2013) with N_{CN} > 15 000 cm^{-3} (right) during the campaign. Bulk CCN activation ratios (AR) at all three supersaturations of 0.2 %, 0.5 % and 0.8 % against N_{CN} in clear days and polluted days are shown in (**a** and **b**) respectively. Diurnal variations of AR, derived κ_{chem} and fraction of total organic mass signal at m/z 44 (f_{44}) are shown in **(c)** (background conditions) and **(d)** (polluted events). Mass concentrations of black carbon (BC), organics, nitrate (NO_3^-), ammonium (NH_4^+), sulfate (SO_4^{2-}), chloride (Cl^-) irons etc. are shown in **(e)** (background conditions) and **(f)** (polluted events). N_{CN} at size range of nucleation, Aitken and accumulated mode are shown in (**g** and **h**) for background conditions and polluted events respectively.

ACPD
14, 14889–14931, 2014

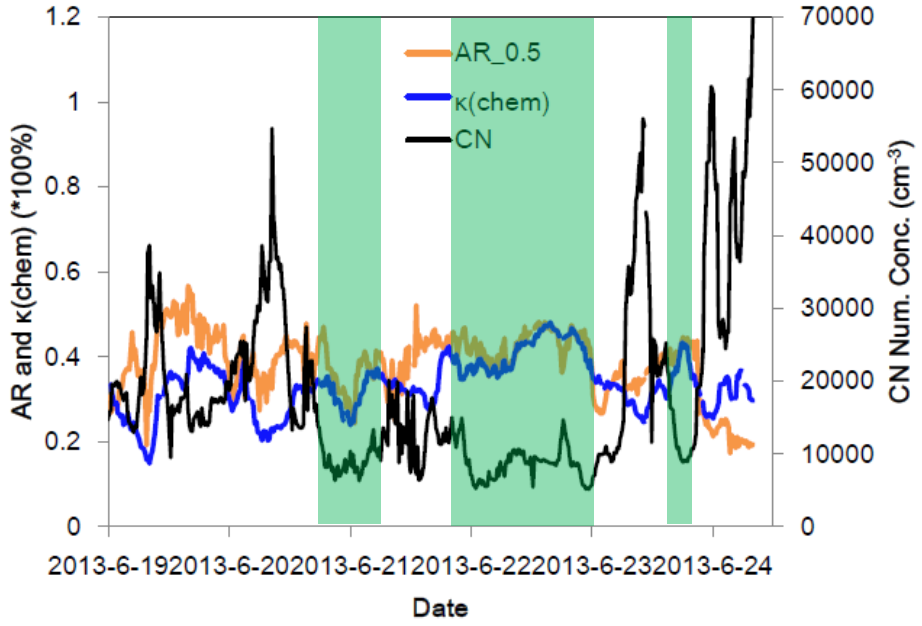

Figure 9. An example for temporal variations of bulk AR at spersaturation of 0.5 %, derived κ_{chem} and N_{CN} during the campaign (19–24 June 2013). The periods (with low N_{CN}) when high correlations between bulk AR and κ_{chem} were observed were marked by rectangles in light green color.

ACPD
14, 14889–14931, 2014